

Characteristics of infrared point sources associated with OH masers *

Ji-Mang Mu^{1,2}, Jarken Esimbek¹, Jian-Jun Zhou¹ and Hai-Juan Zhang^{1,2}

¹ National Astronomical Observatories/Urumqi Observatory, Chinese Academy of Sciences, Urumqi 830011, China; mujm@uao.ac.cn

² Graduate University of Chinese Academy of Sciences, Beijing 100049, China

Received 2009 April 23; accepted 2009 October 25

Abstract We collect 3249 OH maser sources from the literature published up to April 2007, and compile a new catalog of OH masers. We look for the exciting sources of these masers and their infrared properties from IRAS and MSX data, and make a statistical study. MSX sources associated with stellar 1612 MHz OH masers are located mainly above the blackbody line; this is caused by the dust absorption of stellar envelopes, especially in the MSX_A band. The mid-IR sources associated with stellar OH masers are concentrated in a small region in an $[A]-[D]$ vs. $[A]-[E]$ diagram with a small fraction of contamination; this gives us a new criterion to search for new stellar OH masers and distinguish stellar masers from unknown types of OH masers. IR sources associated with 1612 MHz stellar OH masers show an expected result: the average flux of sources with $F_{60} > F_{25}$ increases with increasing wavelength, while those with $F_{60} < F_{25}$ vary little with wavelength, because the sources with $F_{60} < F_{25}$ are much hotter than those with $F_{60} > F_{25}$.

Key words: masers: OH maser — stars: late-type star — catalog — star-forming region — infrared radiation

1 INTRODUCTION

Astrophysical masers play an important role in studying the evolution of star-forming regions and late-type stars. So far, several kinds of masers, including SiO, H₂O, OH, CH₃OH, etc., have been found (Snyder & Buhl 1974; Cheung et al. 1969; Weaver et al. 1965; Barrett et al. 1971). Thousands of these masers have been detected in the past decades; many catalogs of these masers and statistical studies based on them have been published (Engels 1979; Cesaroni et al. 1988; Valdettaro et al. 2001; Chen et al. 2001; Te Lintel Hekkert et al. 1989; Pestalozzi et al. 2007; Val'Tts & Larionov 2007). Recently, the relations of SiO maser emission and H₂O maser emission with mid-IR radiation were studied based on a large sample by Jiang (2002) and Esimbek et al. (2005), but similar work on OH masers was absent. Though more and more OH masers have been found in recent years (Caswell 2004; Edris et al. 2007), there is not a complete updated catalog of OH masers, nor is there a detailed statistical study of OH maser sources and their infrared characteristics.

* Supported by the National Natural Science Foundation of China.

Therefore, it is imperative to collect all OH masers and compile a new up-to-date catalog. IRAS (Infrared Astronomy Satellite) surveyed 98 percent of the whole sky at 12, 25, 60, and 100 μm wavebands and established a point source catalog (PSC); MSX (Midcourse Space Experiment) surveyed the whole Galactic plane at $A(8.28 \mu\text{m})$, $B_1(4.29 \mu\text{m})$, $B_2(4.35 \mu\text{m})$, $C(12.13 \mu\text{m})$, $D(14.65 \mu\text{m})$, and $E(21.34 \mu\text{m})$ wavebands with high sensitivity. These are convenient for us to study the characteristics of infrared sources associated with OH masers and to understand the physical conditions of maser sources. We collected 3249 OH maser sources from the literature which were published up to April 2007. Section 2 describes the sample of OH masers and associated infrared sources. In Section 3, we discuss the color indexes of MSX sources associated with OH masers, the average flux distribution of IR sources and the IR pump of OH masers. A brief conclusion is given in Section 4.

2 SAMPLE

We collect 3249 OH maser emission sources from the literature published up to April 2007 and compile a new catalog. These masers are usually classified into interstellar masers (masers associated with star-forming regions) and stellar masers (masers associated with late-type stars). There are still many OH maser sources whose type is unknown. If one infrared point source is located within 1-arcmin of the maser, we think it is associated with the maser. The numbers of different frequency OH masers associated with infrared point sources are given in Table 1. The total numbers of interstellar, stellar and unknown type OH masers which are associated with IRAS infrared sources are 172 (71% of total interstellar OH masers), 2087 (82% of total stellar OH masers) and 344 (77% of total unknown type OH masers) respectively, and the corresponding numbers for MSX are 197 (82%), 1765 (69%), and 296 (66%). The percentage of interstellar maser sources associated with MSX infrared sources is higher than stellar maser sources; because the sensitivity and spatial resolution of the MSX are high, it can detect the weak infrared sources from star-forming regions with relatively low temperatures. As for stellar and type unknown OH masers, the percentages of OH masers associated with MSX sources compared to the total number are less than those of IRAS sources, because the MSX survey mainly covered the Galactic plane within $|b| \leq 4.5^\circ$ while IRAS surveyed 98 percent of the whole sky. It is evident that many of them have associated IR sources. There are thirteen masers; each one is associated with two IRAS sources and about one hundred masers where each has more than one MSX counterpart due to the higher spatial resolution of MSX data. We selected the nearest and highest quality one as the maser exciting source.

3 RESULTS AND DISCUSSION

3.1 Color Indexes of MSX Sources Associated with OH Masers

We study the IRAS color index of IR sources associated with OH masers in a large sample and get similar results to Chen (2001) and Moore et al. (1988). In the color-color diagram, a large amount of stellar IR sources are below the blackbody line, while nearly all the interstellar IR sources are above the blackbody line and have a characteristic temperature lower than 30 K. We also plot MSX color-color diagrams of the IR sources associated with 1612 MHz OH masers. Figure 1 presents color indexes $[C]-[D]$ vs. $[C]-[E]$ and $[A]-[D]$ vs. $[A]-[E]$. Here, $[C]-[D]$ and $[C]-[E]$ denote $2.5 \log(F_D/F_C)$ and $2.5 \log(F_E/F_C)$. Unlike the IRAS color index, MSX sources associated with stellar 1612 MHz OH masers are mainly distributed above the blackbody line (75% and 91% of the stellar sources are above the blackbody line in Figs. 1(a) and (b) respectively). The reason for this is the absorption of circumstellar dust. Evolution of OH stars leads to O-rich stars with thick dust shells. The silicate absorption features at 9.7 μm and even 18 μm are very important. They correspond to group A OH/IR stars in Chen et al. (2001). Such absorption would make the brightness in the MSX A band faint. Therefore, it is easy to understand why they are mainly located above the blackbody line.

Table 1 OH maser source numbers associated with infrared point sources. The numbers in the brackets are the total number of OH maser sources for the three situations.

	Frequency (MHz)	Number of OH masers (IRAS)	Number of OH masers (MSX)
interstellar	1612	172/(241)	54
	1665		63
	1667		150
	1720		176
stellar	1612	2087/(2562)	1874
	1665		254
	1667		625
	1720		20
type unknown	1612	344/(446)	182
	1665		200
	1667		252
	1720		50

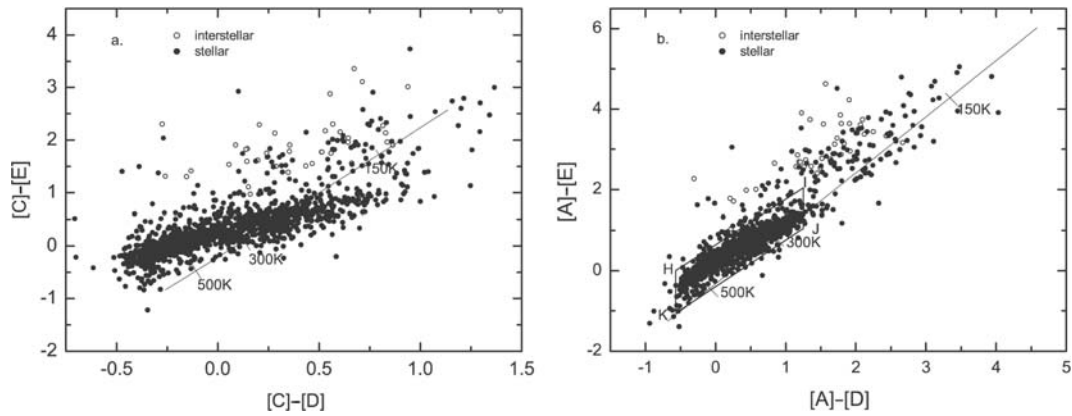


Fig. 1 MSX color-color diagram of (a) $[C]-[D]$ vs. $[C]-[E]$ and (b) $[A]-[D]$ vs. $[A]-[E]$ associated with 1612 MHz OH masers. The solid line shows blackbodies with temperatures from 120 to 1000 K. Positions of H, I, J and K in (b) are $(-0.57, 0.0)$, $(1.25, 2.05)$, $(1.25, 1.05)$ and $(-0.57, -1.0)$.

There are 1356 IR sources associated with 1612 MHz stellar OH masers, 83% of them (1131 sources) are located in a quadrangle area HIJK (see Fig. 1(b)). A statistical study of the IR sources associated with mainline OH masers indicates that about 70% of the IR sources are located in the same region. However, only 3 (6%) of the interstellar sources associated with 1612 MHz OH masers are in this region; the contamination is very small. Therefore, MSX data are suitable for characterizing stellar OH masers. This graph provides us with a new criterion to distinguish stellar OH masers from type unknown OH maser sources and helps us to search for new stellar OH masers. The interstellar sources are relatively dispersed and contaminated by a small portion of stellar sources, so it is hard to distinguish them from the stellar maser sources.

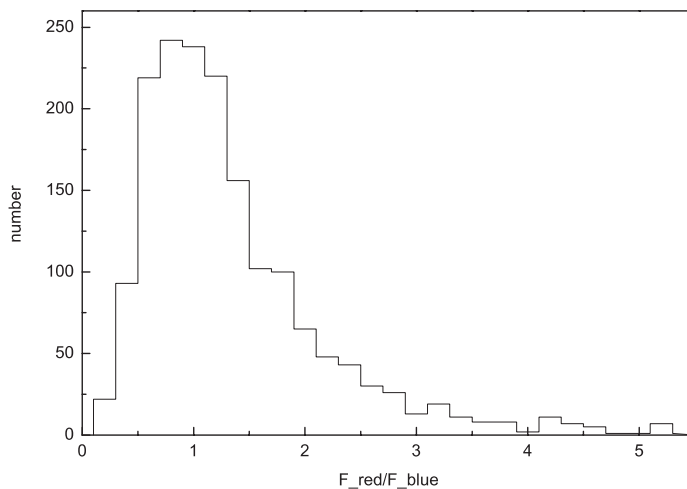


Fig. 2 Distribution of 1612 MHz OH maser peak flux densities of redshifted and blueshifted features for 1727 stellar sources.

3.2 Average Flux Distribution of IR Sources Associated with OH Masers

About 86% of 1612 MHz stellar OH maser stars show a double peaked spectrum. The difference of flux density between redshifted and blueshifted features (Fig. 2) indicates that the number of 1612 MHz stellar masers with stronger blueshifted features is nearly the same as that of sources with stronger redshifted features. This result, based on a larger sample, agrees with previous results (Gray et al. 2008). The flux density ratio of blueshifted to redshifted features was determined by the complex condition of the stellar envelope and pump mechanism (Collison & Fix 1992; Spaans & Van Langevelde 1992; Gray et al. 2008). The study of Tang et al. (2008) shows that the observed fact that the 1612 MHz maser fades over a timescale of decades proves that the appearance or disappearance of the maser is exchangeable with respect to one source; the appearance or disappearance of one of the two peaks in one source is also exchangeable. The phenomenon that sometimes only one peak appears or one of the two peaks is weak may be explained by the relatively thin circumstellar shell, which brings a relatively short amplification path for the maser. More theoretical work is needed to properly explain the asymmetry of the 1612 MHz stellar OH maser spectrum.

Figure 3 displays the average flux density of IR sources associated with interstellar (averaging 50 sources) and stellar 1612 MHz OH masers. Four IRAS wavebands (12, 25, 60 and $100 \mu\text{m}$) and four MSX wavebands (*A*, *C*, *D* and *E*) were used to plot the diagram. The average flux density increases with the increase of wavelength, because the interstellar IR sources are usually embedded in molecular clouds which have low temperatures and lead to long wavelength emission. The average flux increases with wavelength for stellar sources just as for interstellar sources. However, stellar sources often have relatively high temperatures: radiation with short wavelengths should be stronger than that with long wavelengths. To understand what is happening, we divide the stellar sources into two types: sources with $F_{60} > F_{25}$ (490 sources, F_{60} and F_{25} denote the flux densities of $60 \mu\text{m}$ and $25 \mu\text{m}$ respectively) and sources with $F_{60} < F_{25}$ (910 sources). The average flux of the former increases with increasing wavelength and the latter is otherwise. The average flux of different IR wavelengths for the sources with $F_{60} < F_{25}$ varies relatively little. The difference comes from the dust temperature of the circumstellar shell. The sources with $F_{60} < F_{25}$ are much hotter than those with $F_{60} > F_{25}$; this leads the average flux of the two kinds of sources to vary differently with respect to wavelength.

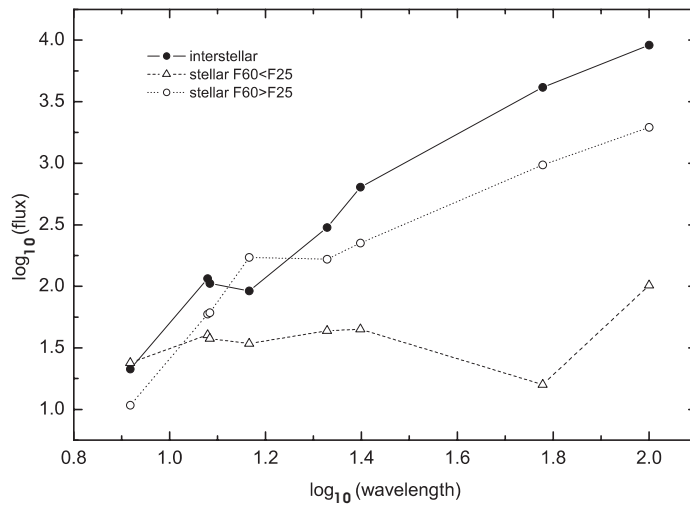


Fig. 3 Average flux density of IR sources associated with 1612 MHz (50 sources) interstellar OH masers and with 1612 MHz stellar OH masers of F60 < F25 (910 sources), and F60 > F25 (490 sources). MSX and IRAS data are available for all sources.

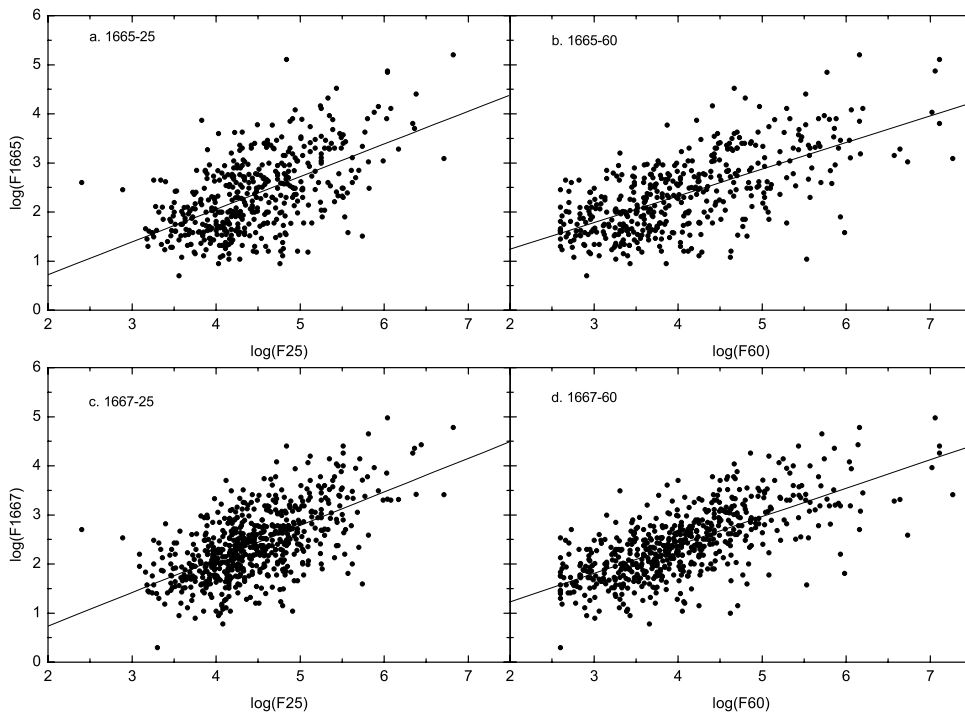


Fig. 4 (a) Peak flux density of 1665 MHz stellar OH maser vs. 25 μm flux density; (b, c, d) Same as (a) but 1665 MHz vs. 60 μm , 1667 MHz vs. 25 μm and 1667 MHz vs. 60 μm . Solid lines are linear fitting lines.

3.3 Infrared Radiation and Maser Pump

It has long been accepted that far-infrared pumping of the OH 1612 MHz line is feasible in type II OH/IR stars (Elitzur et al. 1976; He 2005). The linear correlation coefficients between 1612 MHz stellar OH maser emission and the associated IRAS source radiation at 12, 25, 60 and 100 μm are 0.26, 0.39, 0.28, and 0.10 respectively; such small correlation coefficients suggest that infrared radiation at 12, 25, 60 and 100 μm does not work or just plays a small role in pumping 1612 MHz stellar OH masers. This agrees with the result that infrared radiation at 35 and 53 μm pumps 1612 MHz stellar OH masers (Elitzur et al. 1976; He 2005). However, the situation of stellar mainline OH masers is completely different. The correlation coefficients of F25-F1665, F60-F1665, F25-F1667 and F60-F1667 (F1665 and F1667 denote the flux densities of 1665 and 1667 MHz OH masers) are 0.57, 0.65, 0.61 and 0.70 respectively (Fig. 4). The corresponding empirical relations are:

$$\log(\text{F1665}) = -0.606(0.204) + 0.666(0.045)\log(\text{F25});$$

$$\log(\text{F1665}) = 0.153(0.124) + 0.544(0.030)\log(\text{F60});$$

$$\log(\text{F1667}) = -0.628(0.160) + 0.683(0.035)\log(\text{F25});$$

$$\log(\text{F1667}) = 0.071(0.099) + 0.579(0.024)\log(\text{F60}).$$

The strong correlations indicate that the far-IR radiation at 25 and 60 μm may play an active role in pumping mainline OH masers of late-type stars.

For interstellar masers, the linear correlation coefficients of F12–F1612, F25–F1612, F60–F1612, and F100–F1612 are 0.33, 0.38, -0.02 and 0.40 respectively; the correlation is also not strong, especially for F60–F1612. The pumping mechanism of the 1612 MHz interstellar OH maser is very complex; it may involve four alternative scenarios or their combinations: absorption by quiet OH cloudlets, different OH maser pump mechanisms, competitive gain between mainline and 1612 MHz masers, and anisotropy of the maser emission (He 2005). The correlation coefficients are 0.36, 0.35, 0.39, 0.34, 0.43 and 0.40 for F25–F1665, F25–F1667, F60–F1665, F60–F1667, F100–F1665 and F100–F1667, respectively. These medium correlations indicate that infrared radiation at 12, 25, 60 and 100 μm works in the pumping of interstellar OH masers, but the correlation coefficients seem to increase with wavelength; the longer wavelength radiation may be more effective in pumping interstellar mainline OH masers. One should keep in mind that this is just a tentative conclusion; more infrared data at longer wavelengths are needed to verify it.

4 CONCLUSIONS

We have collected 3249 OH maser sources and compiled a new catalog, which includes all OH masers found up to April 2007. We selected infrared sources within 1' of the maser from the IRAS and MSX point source catalog as the exciting sources. Some interesting results were drawn from the statistical study. Unlike the IRAS color index, MSX sources associated with stellar OH masers are mainly above the blackbody line; this means that the absorption of circumstellar dust makes the brightness in the MSX_A band faint. The mid-IR sources associated with stellar OH masers are concentrated in a small region in an $[A]-[D]$ vs. $[A]-[E]$ diagram with a small fraction of contamination; this gives us a new criterion to search for new stellar OH masers and distinguish stellar OH masers from unknown type OH maser sources. We find that the average flux of IR sources associated with 1612 MHz stellar OH masers increases with increasing wavelength; to understand the reason for this, we divide the sources into two types according to the relation of flux densities of 25 μm and 60 μm . The study shows that the average flux of sources with $\text{F60} > \text{F25}$ increases with increasing wavelength because of the low temperature of the circumstellar shell, while sources with $\text{F60} < \text{F25}$ are much hotter than those with $\text{F60} > \text{F25}$, so the average flux varies little with wavelength.

Acknowledgements We thank Professor Xing-Wu Zheng for his constructive discussion. This work is supported by the National Natural Science Foundation of China (Grant Nos. 10778703 and 10873025) and the Program of the Light in China's Western Region (LCWR) (Nos. RCPY200605 and RCPY200706).

References

- Barrett, A. H., Schwartz, P. R., & Waters, J. W. 1971, *ApJ*, 168, L101
Caswell, J. L. 2004, *MNRAS*, 349, 99
Cesaroni, R., Palagi, F., Felli, M., Catarzi, M., Comoretto, G., et al. 1988, *A&AS*, 76, 445
Chen, P. S., Szczerba, R., Kwok, S., & Volk, K. 2001, *A&A*, 368, 1006
Cheung, A. C., Rank, D. M., Townes, C. H., Thornton, D. D., & Welch, W. J. 1969, *Nature*, 221, 626
Collison, A. J., & Fix, J. D. 1992, *ApJ*, 390, 191
Edris, K. A., Fuller, G. A., & Cohen, R. J. 2007, *A&A*, 465, 865
Elitzur, M., Goldreich P., & Scoville, N. 1976, *ApJ*, 205, 384
Engels, D. 1979, *A&AS*, 36, 337
Esimbek, J., Wu, Y. F., & Wang, J. Z. 2005, *ChJAA (Chin. J. Astron. Astrophys.)*, 5, 587
Gray, M. D., Howe, D. A., & Lewis, B. M. 2008, *MNRAS*, 391, 334
He, J. H. 2005, *New Astronomy*, 10, 283
Jiang, B. W. 2002, *ApJ*, 566, L37
Moore, T. J. T., Cohen, R. J., & Mountain, C. M. 1988, *MNRAS*, 231, 887
Pestalozzi, M. R., Chrysostomou, A., Collett, J. L., Minier, V., Conway, J., & Booth, R. S. 2007, *A&A*, 463, 1009
Spaans, M., & Van Langevelde, H. J. 1992, *MNRAS*, 258, 159
Snyder, L. E., & Buhl, D. 1974, *ApJ*, 189, L31
Tang, X., Jiang, B. W., & Fu, J. N. 2008, *AJ*, 135, 1681
Te Lintel Hekkert, P., Versteeg-Hensel, H. A., Habing, H. J., & Wiertz, M. 1989, *A&AS*, 78, 399
Valdettaro, R., Palla, F., Brand, J., Cesaroni, R., et al. 2001, *A&A*, 368, 845
Larionov, G. M., & Val'Ts, I. E. 2007, *Astronomy Reports*, 51, 756
Weaver, H., Williams, D. R. W., Dieter, N. H., & Lum, W. T. 1965, *Nature*, 208, 29